Applied Catalysis A: General 408 (2011) 73–77

Contents lists available at SciVerse ScienceDirect

Applied Catalysis A: General

journal homepage: www.elsevier.com/locate/apcata

Immobilization of enzymes into self-assembled iron(III) hydrous oxide nano-scaffolds: A bio-inspired one-pot approach to hybrid catalysts

Martín G. Bellino[a,*], Alberto E. Regazzoni[a,b]

[a] Gerencia Química, Centro Atómico Constituyentes, Comisión Nacional de Energía Atómica, Av. General Paz 1499, B1650KNA San Martín, Argentina
[b] Instituto Jorge A. Sabato, Universidad Nacional de San Martín, Av. General Paz 1499, B1650KNA San Martín, Argentina

ARTICLE INFO

Article history:
Received 28 June 2011
Received in revised form 6 September 2011
Accepted 11 September 2011
Available online 16 September 2011

Keywords:
Biocatalysts
α-Amylase
Immobilization
Hybrid nanoparticles
Iron (hydrous)oxide

ABSTRACT

A simple bio-inspired one-pot procedure for the immobilization of α-amylase into maturing hybrid iron(III) hydrous oxide nanostructures is described. The method resorts to the urease mediated decomposition of urea to induce the homogeneous precipitation of amylase-iron(III) hydrous oxide ensembles. Appropriate setting of the synthesis parameters, which control the shape and texture of the resulting hybrid nanostructures, is key to amylase entrapment. Highly efficient hybrid catalysts were prepared at the lowest urease concentration (0.5 mg/mL), where spherical 100 nm size hybrid iron(III) hydrous oxide ensembles formed; their amylase load depended on the enzyme concentration, in a michaelian fashion. Their specific activity is nearly that of free amylase. These catalysts are reusable, with no loss of performance, and substantially more active than the free enzyme at extreme pHs and temperatures. The high efficiency of the hybrid ensembles is ascribed to their open structure, high enzyme loading, and negligible amylase inactivation.

1. Introduction

Many existing and emerging bio-assisted processes benefit from the immobilization of enzymes in inorganic supports. In these functional materials, the enzymes furnish high specificity and efficient chemical conversion, whereas the supports provide the means for enzyme re-utilization, thus extending its operative lifetime. Suitable supports open, in addition, the possibility of integrating the specificity of the enzymes into sensing devises. Current applications include industrial processes, waste treatments, pharmaceutical products, and biosensors [1–4]. Mesoporous powders [5–10] and sol–gel matrices [11–14] represent two of the most widely used inorganic scaffolds for achieving this type of bio-active systems. The synthesis of bio-functionalized mesoporous materials use a multiple-step approach to combine the properties that arise from tailored confined spaces and enzymatic activity. The materials obtained by typical protocols suffer however important drawbacks, including poor enzyme loading and high enzyme leaching during the enzymatic reaction [5–9]. A common procedure to reduce enzyme leaching is covalent post-immobilization, at the cost of additional synthesis steps. Yet, the most important penalty paid by covalent post-immobilization is the alteration of the structural conformation of the anchored enzymes [4,15,16]. Sol–gel encapsulation offers a different approach, resorting to entrapment (via inclusion) of the enzymes during the chemical synthesis of silica gels. Although this method avoids some of the aforementioned problems, the rather aggressive requirements of conventional synthesis procedures (e.g., harsh co-solvents, poisonous catalysts) pose severe restrictions to the type of enzyme that can be immobilized [4,17,18]. Recently, it was shown that the polypeptide silaffin, from diatoms, provides mild conditions for the encapsulation of enzymes within bio-silica, thus granting high enzymatic activity [19].

In nature, a large number of microorganisms produce biominerals by hydrolyzing secreted urea to carbonate and ammonium to prompt intra- or extra-cellular precipitation [20,21]. Mimicking nature, it was recently demonstrated that a wide variety of nanostructured materials can be synthesized by homogeneous precipitation from salt solutions that are being alkalinized by the decomposition of urea catalyzed by urease [22–27]. Considering the benign synthesis conditions of this biomimetic approach, and bearing in mind that enzymes should anchor themselves to growing metal oxide particles, one-pot enzyme immobilization procedures can be envisaged (see sketch in Fig. 1). As a proof of the feasibility of this reasoning, this communication shows that α-amylase can be indeed immobilized into maturing iron hydrous oxide nanostructures, and that the resulting hybrid catalysts gain in performance as compared to the free enzyme.

Iron (hydr)oxide was selected because its potential biomedical applications [28–30], whereas amylase, a well-known enzyme, was chosen for its variety of uses that span from the treatment of effluents to pharmaceutical applications [31–33].

* Corresponding author. Tel.: +54 11 6772 7958.
E-mail address: mbellino@cnea.gov.ar (M.G. Bellino).

0926-860X/$ – see front matter © 2011 Elsevier B.V. All rights reserved.
doi:10.1016/j.apcata.2011.09.008

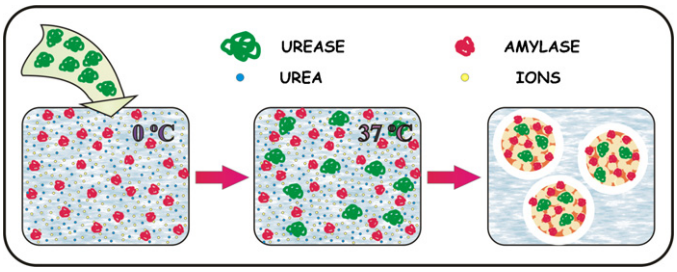

Fig. 1. Sketch illustration of the formation of bio-functional hybrid nanostructures during urease mediated decomposition of urea.

2. Experimental

2.1. Preparation and characterization of the hybrid catalysts

Freshly prepared $FeCl_2$, urea and α-amylase solutions were mixed in appropriate proportions; the resulting solution was cooled down in an ice-water bath. Then, a pre-cooled solution of urease was added rapidly, and mixed under vigorous stirring; the final volume was 10 mL. Afterwards, the solution was incubated at 37 °C for 3 h under continuous stirring. Finally, the formed precipitates were separated by centrifugation, washed thoroughly with water, and re-suspended in 10 mL of water. The concentrations of $FeCl_2$ and urea in the reacting systems were 0.05 and 0.2 M, respectively, whereas the concentrations of urease and amylase were spanned between 0.5 and 2.5 mg/mL, and 1 and 2 mg/mL, respectively. All supernatants were stored for analyses.

Syntheses were carried out using thoroughly cleaned capped glass bottles. $FeCl_2.4H_2O$ and urea were analytical grade reagents. Urease (from Jack bean) and α-amylase (from Bacillus Species) were purchased from Sigma–Aldrich; their activities, as declared by the vendor, are 956 and 1.0 units/mg, respectively. All solution were made up using deionized water (conductivity less than 0.1 μS/cm), and filtered through 200 nm pore size membranes.

The obtained precipitates were characterized by FE-SEM and TEM using a Zeiss Leo 982 Gemini and a Philips EM-301 electron microscopes. ED patterns were acquired using a Philips EM-301 instrument. XRD patterns were obtained using a Philips PW3710 apparatus.

2.2. Determination of the enzymatic activity

The enzymatic activity of immobilized α-amylase was determined by the well known starch – iodine colorimetric method [34,35]. Briefly, a measured volume (typically 50 μL) of the aqueous suspension containing the synthesized hybrid catalyst was added to 10 mL of a 2% starch solution (soluble starch from potato). After a given time, the reaction was quenched by addition of a stoichiometric (with respect to the initial starch concentration) amount of iodine. Then, the solution was diluted with an appropriate water volume, and the absorbance was read at 620 nm in a Hewlett-Packard 8453 spectrophotometer; dilutions were made as necessary. Blank measurements, i.e., in the absence of α-amylase, were carried out as before. The mass of degraded starch was then calculated from: $DS = (Abs_B - Abs_S)/Abs_B \times M$, where Abs_B and Abs_S are the absorbance of the blank and the sample, respectively, and M is the mass of starch in the initial solution. The pH of the reacting solutions was fixed by small additions of HCl or NaOH. All runs were carried out in triplicate at a constant temperature, using a water bath.

In selected cases, re-use experiments were also carried out. After each test, performed as described above, the hybrid catalyst particles were removed by centrifugation from the reaction vessel, washed thoroughly with water, and re-suspended in 10 mL of a fresh starch solution.

The amount of immobilized α-amylase was assessed deriving the concentration of the enzyme in the supernatant solutions from measured activity values, and solving the mass balance of the systems.

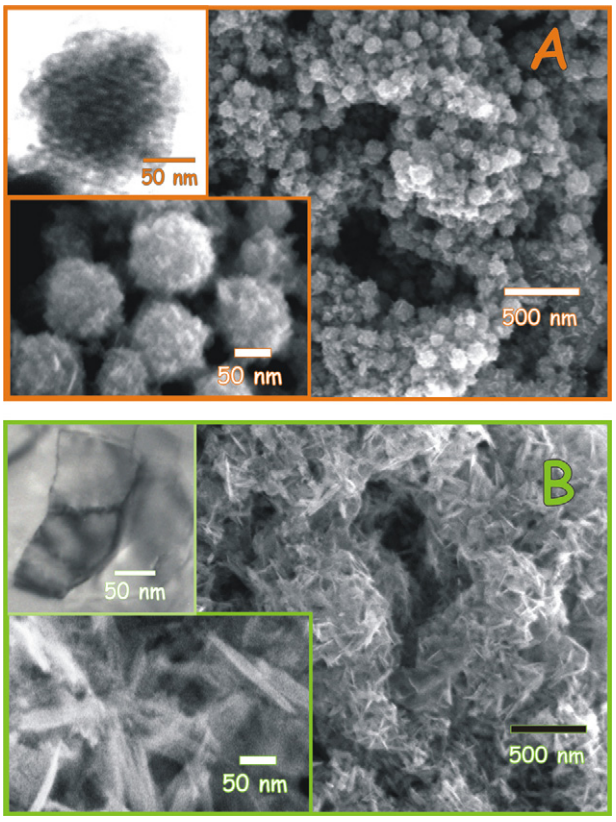

Fig. 2. Morphology of amylase-functionalized iron hydrous oxide nanostructures prepared by aging oxygen saturated 0.05 M $FeCl_2$ solutions containing 1 mg/mL amylase, 0.2 M urea, and different concentrations of urease for 3 h at 37 °C: (A) 0.5 mg/mL and (B) 2.5 mg/mL. The insets show blow-ups of the FE-SEM images, and TEM micrographs.

3. Results and discussion

Incubation of oxygen-saturated solutions containing amylase (1 mg/mL), iron(II) chloride (0.05 M), urea (0.2 M) and urease at 37 °C leads to the precipitation of different iron hydrous oxides. As the incubation proceeds, hydrolysis of urea (catalyzed by urease) provides the necessary amount of base that triggers the formation of the solid phase. Depending on the concentration of urease, the pH of the reacting solutions evolved from 6 to about 8, thus granting complete precipitation. Concomitant immobilization of amylase (see below) eventually takes place as sketched in Fig. 1. The nature of the precipitated iron hydrous oxide nanoparticles depends strongly on the amount of added urease. At the lowest urease concentration (0.5 mg/mL), a steady development of a red-brownish turbidity, typical of iron(III) (hydr)oxides, was evident. The obtained solid is composed of 100 nm spherical nanostructures made up by ca. 5 nm size nanoparticles (Fig. 2A). These self-assembled nanostructures, which are amorphous as revealed by electron diffraction and XRD (see Supplementary data, Figs. S1 and S2), have an evident open structure that resembles that of mesoporous materials (see TEM image in the inset of Fig. 2A). At the highest explored urease concentration (2.5 mg/mL), on the other hand, a greenish solid precipitated readily. This is composed

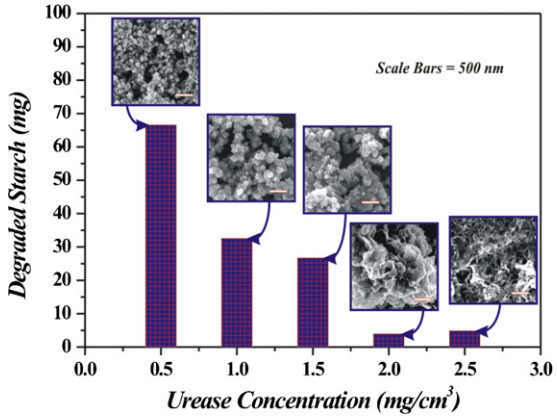

Fig. 3. Influence of urease concentration on the activity of the hybrid catalysts at pH 6 and 20 °C; volume of hybrid catalysts dispersion: 50 μL; volume of 2% starch solution: 10 mL; reaction time: 5 min. Inserted micrographs depict the morphologies of the different nano-scaffolds.

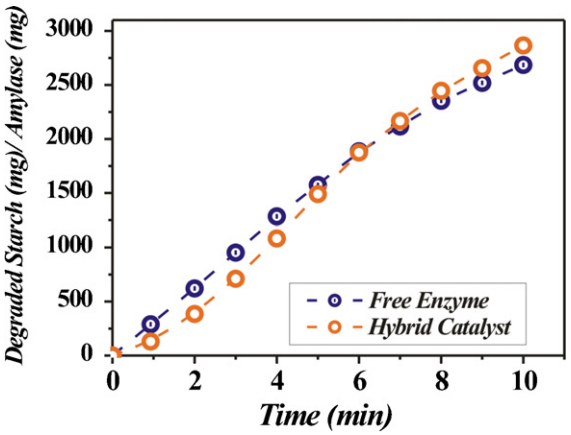

Fig. 4. Degradation of starch by free amylase and by the hybrid catalyst shown in Fig. 2A; volume of 1 mg/mL free amylase solution: 50 μL; volume of hybrid catalyst dispersion: 50 μL; volume of 2% starch solution: 10 mL; T = 20 °C; pH 6.0. Note that data are reported as mg degraded starch per mg amylase.

of aggregates of hexagonal plate-like particles (Fig. 2B), a crystalline habit that is typical of green-rust (a Fe(II)-Fe(III) layered double hydroxide [36–38]), which upon drying in air turned into lepidocrocite and goethite (see Supplementary data, Fig. S2). The influence of urease on the nature of the synthesized iron hydrous oxides is due to the interplay of the rates of urea hydrolysis and iron(II) oxidation. At low urease concentrations, the rate of iron(II) oxidation surpasses the pace of base production, thus iron(II) is oxidized in solution and iron(III) (hydr)oxides nucleate homogeneously. At high urease concentrations, urea hydrolysis takes place rapidly and precipitation of iron(II) hydroxide ensues; the solid is latter oxidized to green-rust phases [39,40]. Interestingly, the absence of amylase does not alter the overall morphology of the obtained precipitates (see Supplementary data, Fig. S3).

These amylase-functionalized nanostructures have strikingly different abilities to degrade starch (Fig. 3). At pH 6, the spherical nanostructure degraded ca. 14 times more starch than the hexagonal plate-like aggregates. The unlike reactivities of these nanostructures may in principle be traced back to their notably dissimilar textures, which should influence their ability to immobilize active amylase; particle texture determines the number of anchoring OH sites, as well as their availability [41,42]. In fact, the spherical nanostructure, which hosts 170 mg amylase/g, takes up about three times more amylase than the hexagonal plate-like aggregates (49 mg amylase/g). Competition by urease should not be disregarded. More importantly, the latter figres indicate that immobilization of amylase into the hexagonal plate-like aggregates produces inactivation. In what follows, the attention shall be centered on the activity of the spherical nanostructures obtained at the lowest urease concentration, which should be regarded as a hybrid ensemble in which the amorphous 5 nm size iron(III) (hydr)oxide nanoparticles are held together by the chemisorbed proteins, as well as by London – van der Waals forces.

The kinetic profiles of starch degradation by the free and by the immobilized enzyme are compared in Fig. 4. Clearly, immobilization of amylase into the self-assembled spherical nanostructure has a very slight effect on its overall enzymatic activity. A short induction period can however be noted. For this reason, the specific activity values reported hereafter are cast in terms of mg degraded starch per mg amylase @ 5 min; they should not be confused with initial reaction rates. Importantly, the specific activity of the immobilized amylase is 0.95 times that of the free enzyme.

Whether the allosteric-like behavior perceived in Fig. 4 is the result of diffusional effects is dim. Usually, related bio-functionalized systems, such as enzymes supported on mesoporous micrometric powders or encapsulated in sol–gel matrices, bear decreased specific activities, owing to mass-transfer limitations. For instance, the relative activity (i.e., the ratio of the specific activities of the immobilized and free enzymes) of amylase supported on mesoporous silicas ranges between 0.3 and 0.9, depending on pore size [5], whereas the specific activity of amylase encapsulated in silica xerogels is a fifth of that of free amylase [14]. Clearly, the amylase-functionalized iron(III) hydrous oxide nanostructure prepared by the one-pot procedure advanced here does not suffer of such a penalty. Apparently, the evident open structure of the hybrid ensembles (see TEM image in the inset of Fig. 2A) allows the free transport of the substrate molecules.

The self-assembled hybrid network of iron(III) hydrous oxide nanoparticles should also allow high enzyme loadings. To assess whether the enzymatic activity of the synthesized spherical nanostructures stems from adsorbed or entrapped amylase, the following experiment was performed. First, iron(III) hydrous oxide nanoparticles were prepared as described, but in the absence of amylase. Then, the resulting precipitate was re-suspended in 1 mg/mL amylase solution and incubated for 3 h. This two-steps synthesis protocol yielded a loading of 24 mg amylase/g, which is seven-fold lower than that obtained following the proposed one-pot procedure. In addition, the specific activity of the so-obtained material was a tenth of that of the nanostructures formed by one-step functionalization. Summing up, the two-steps process produced a material that is about two orders of magnitude less efficient. This result stresses the importance of amylase entrapping during the formation of the iron(III) hydrous oxide hybrid nanostructure, a condition that it is granted by the one-pot immobilization procedure proposed here.

Another limitation of bio-functionalized materials prepared by conventional sol–gel encapsulation procedures and post-functionalization of mesoporous micrometric powders is the rather low enzyme loadings that can be attained; typically, they amount to 0.1–5% (w/w) [5–8,16]. The one-pot immobilization procedure described here allows loadings as high as 220 mg amylase/g (i.e., ca. 20%, w/w), matching the highest enzyme loadings exceptionally reported in the literature [10,17]. The load of amylase, which can be tuned by setting the concentration of amylase used in the synthesis, increases with amylase concentration in a michaelian fashion (Fig. 5). The specific activity of the functionalized nanostructures however decreases, albeit slightly, with increasing amylase loadings (Fig. 5), probably due to inactivation by packing [43]. Nevertheless, the net efficiency (i.e., mg degraded starch per g catalyst per min) of these materials increases with the load. Clearly,

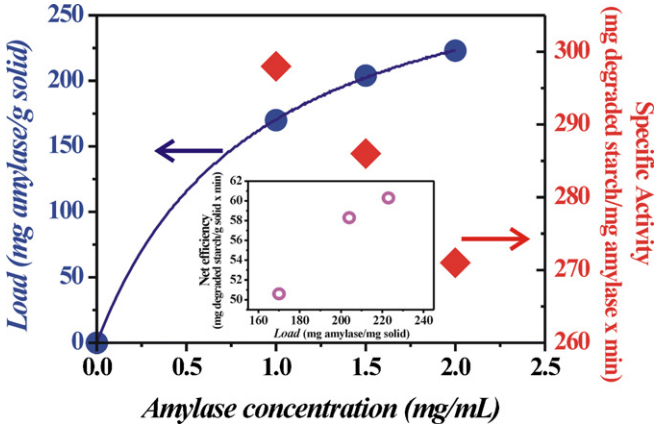

Fig. 5. Amount of amylase immobilized by the iron(III) hydrous oxide spherical nanostructures and specific activity of the hybrid catalysts at pH 6.0 and 20 °C as a function of the concentration of amylase used for functionalization. The inset shows the net efficiency of the hybrid catalysts as a function of amylase loading. Note that the specific activity of free amylase is 315 mg degraded starch per mg amylase per min.

the combination of high specific activities and significant loadings makes the hybrid catalysts prepared by the present bio-inspired one-pot immobilization procedure promising.

Immobilization of amylase provides a very simple way of recovering the enzyme, which can be utilized in subsequent reaction cycles, thus improving its overall performance. Fig. 6, which shows that the hybrid catalyst remains highly active after 5 reaction cycles, indicates that amylase does not deteriorate on repeated use, nor it detaches from the hybrid iron(III) hydrous oxide ensemble.

Free enzymes are active in rather narrow temperature and pH ranges. Immobilization of amylase may in addition prevent unfolding [5,44,45], which should render the enzyme apt to be exploited in much broader ranges. Fig. 7A and B shows that this is indeed the case. As a consequence of the stabilizing effect of immobilization, which buffers the influence of pH and temperature, the activity of the supported enzyme becomes significantly higher than that of free amylase at extreme conditions; e.g., at pH 4, the specific activity of amylase in the hybrid ensemble is nearly 6 times larger (Fig. 7A).

The fate of urease deserves a brief comment. During the synthesis of the hybrid catalyst, urease becomes as well entrapped within the assembling structure of iron(III) hydrous oxide nanoparticles. This was confirmed by reacting the synthesized catalyst with 0.1 M urea solution; a fast rise in pH, from 5.0 to 6.5, was observed.

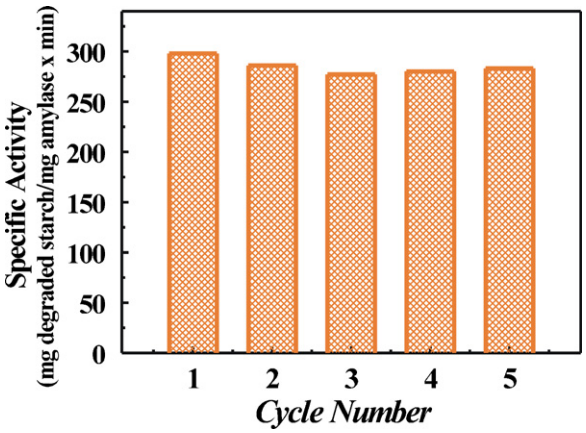

Fig. 6. Specific activity of the functionalized nanostructure shown in Fig. 2A on repeated use; $T = 20\,^{\circ}C$; pH 6.0.

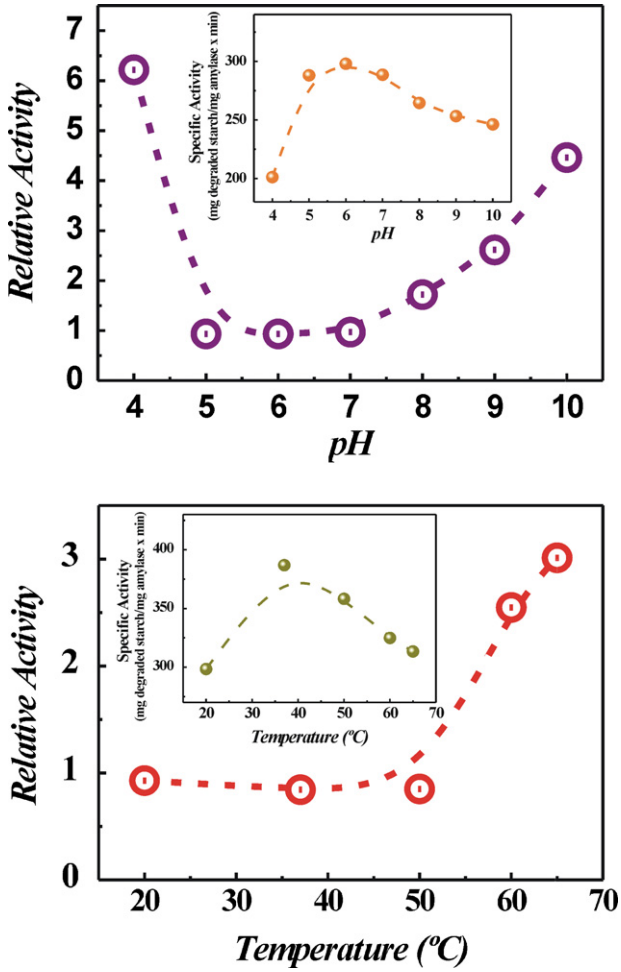

Fig. 7. Influence of pH and temperature on the specific activity of the functionalized nanostructure shown in Fig. 2A relative to that of free amylase; in (A) $T = 20\,^{\circ}C$ and in (B) pH 6.0. The insets show the specific activity of the hybrid catalyst. Dotted lines are guides to the eye.

This result is not surprising, because enzyme entrapping should not be, in principle, selective. Although no especial effort was made to assess the load of urease in the hybrid catalysts, neither its specific activity, the outcome of this result is clear: the bio-inspired one-pot procedure proposed here can be envisaged as a very simple way of immobilizing a consortium of enzymes in a single scaffold.

4. Conclusion

In summary, this work shows that highly efficient hybrid catalysts can be prepared by immobilizing amylase within the self-assembling nanostructures that are being formed during the biomimetic homogeneous precipitation of iron(III) hydrous oxide nanoparticles. Our results demonstrate that appropriate control of the synthesis parameters allows tuning the nature and architecture of the inorganic supports, which in turn determines the overall enzymatic activity of the hybrid catalysts. The excellent performance of the obtained functional hybrid spheres must be attributed to the combination of their open structure, high enzyme loadings and negligible amylase inactivation. Clearly, the benign synthesis conditions provided by the present bioinspired one-pot immobilization method minimize enzyme denaturalization.

This simple procedure can in principle be applied, in a nearly straightforward way, to immobilize a wide variety of enzymes into an assortment of inorganic supports, which would launch the

production of a diversity of new functional hybrid nanostructures for advanced applications. Furthermore, the green nature of these hybrid catalysts makes them promising for waste treatment, environmental remediation, as well as for pharmaceutical and other industrial processes.

Acknowledgments

Partial support by CONICET (PIP-03274) and ANPCyT (PICT-00335 and PICT 1848) is acknowledged. M. G. B. and A. E. R. are members of CONICET. Thanks are due to Centro de Microscopías Avanzadas (FCEN-UBA) for the electron micrographs.

Appendix A. Supplementary data

Supplementary data associated with this article can be found, in the online version, at doi:10.1016/j.apcata.2011.09.008.

References

[1] A.M. Klibanov, Science 219 (1983) 722–727.
[2] G.F. Bickerstaff (Ed.), Immobilization of Enzymes and Cells, Humana Press, Totowa, NJ, 1997.
[3] W. Tischer, V. Kasche, Trends Biotechnol. 17 (1999) 326–335.
[4] B.-W. Park, D.-Y. Yoon, D.-S. Kim, Biosens. Bioelectron. 26 (2010) 1–10.
[5] H.P. Pandya, R.V. Jasra, B.L. Newalkar, P.N. Bhatt, Micropor. Mesopor. Mater. 77 (2005) 67–77.
[6] J.F. Diaz, K.J.J. Balkus, J. Mol. Catal. B 2 (1996) 115–126.
[7] C. Lei, Y. Shin, J. Liu, E.J. Ackerman, J. Am. Chem. Soc. 124 (2002) 11242–11243.
[8] L. Washmon-Kriel, V.L. Jimenez, K.J. Balkus, J. Mol. Catal. B 10 (2000) 453–469.
[9] H.H.P. Yiu, P.A. Wright, N.P. Botting, Micropor. Mesopor. Mater. 44 (2001) 763–768.
[10] H. Takahashi, B. Li, T. Sasaki, C. Miyazaki, T. Kajino, S. Inagaki, Chem. Mater. 12 (2000) 3301–3305.
[11] S. Braun, S. Rappoport, R. Zusman, D. Avnir, M. Ottolenghi, Mater. Lett. 10 (1990) 1–5.
[12] P. Johnson, T.L. Whateley, J. Colloid Interface Sci. 37 (1971) 557–563.
[13] M.T. Reetz, A. Zonta, J. Simpelkamp, Angew. Chem. Int. Ed. 34 (1995) 301–303.
[14] L.E. Vera-Avila, E. Morales-Zamudio, M.P. Garcia-Camacho, J. Sol Gel Sci. Technol. 30 (2004) 197–204.
[15] C.H. Lee, C.Y. Mou, S.C. Ke, T.S. Lin, Mol. Phys. 104 (2006) 1635–1641.
[16] E. Serra, A. Mayoral, Y. Sakamoto, R.M. Blanco, I. Díaz, Micropor. Mesopor. Mater. 114 (2008) 201–213.
[17] I. Gill, A. Ballesteros, J. Am. Chem. Soc. 120 (1998) 8587–8598.
[18] D. Avnir, Acc. Chem. Res. 28 (1995) 328–334.
[19] H.R. Luckarift, J.C. Spain, R.R. Naik, M.O. Stone, Nature Biotechnol. 22 (2004) 211–213.
[20] K.L. Bachmeier, A.E. Williams, J.R. Warmington, S.S. Bang, J. Biotechnol. 93 (2002) 171–181.
[21] S. Stocks-Fischer, J.K. Galinat, S.S. Bang, Soil Biol. Biochem. 31 (1999) 1563–1571.
[22] I. Sondi, S.D. Skapin, B. Salopek-Sondi, Cryst. Growth Des. 8 (2008) 435–441.
[23] S. Vial, J. Ghanbajab, C. Forano, Chem. Commun. (2006) 290–292.
[24] R. de la Rica, H. Matsui, Angew. Chem. Int. Ed. 47 (2008) 5415–5417.
[25] I. Ortega, M. Jobbágy, M.L. Ferrer, F. del Monte, Chem. Mater. 20 (2008) 7368–7370.
[26] S.D. Sÿkapin, I. Sondi, Cryst. Growth Des. 5 (2005) 1933–1938.
[27] C. Pejoux, R. de la Rica, H. Matsui, Small 6 (2010) 999–1002.
[28] S. Laurent, S. Boutry, I. Mahieu, L. van der Elst, R.N. Muller, Curr. Med. Chem. 19 (2009) 4712–4727.
[29] A.K. Gupta, M. Gupta, Biomaterials 18 (2005) 3995–4021.
[30] M. Auffan, J. Rose, J.-Y. Bottero, G.V. Lowry, J.-P. Jolivet, M.R. Wiesner, Nature Nanotechnol. 4 (2009) 634–641.
[31] H. Uhlig, E.M. Linsmaier-Bednar, Industrial Enzymes and their Applications, John Wiley & Sons, New York, 1998.
[32] A. Illanes, Enzyme Biocatalysis: Principles and Applications, Springer, Dordrecht, 2008.
[33] S. Sivaramakrishnan, D. Gangadharan, K.M. Nampoothiri, A. Pandey, Food Technol. Biotechnol. 44 (2006) 173–184.
[34] B.W. Smith, J.H. Roe, J. Biol. Chem. 179 (1949) 53–59.
[35] B.W. Smith, J.H. Roe, J. Biol. Chem. 227 (1957) 357–362.
[36] B.C. Christiansen, T. Balic-Zunic, P.-O. Petit, C. Frandsen, S. Mørup, H. Geckeis, A. Katerinopoulou, S.L. Svane-Stipp, Geochim. Cosmochim. Acta 73 (2009) 3579–3592.
[37] T. Sugimoto, E. Matijević, J. Colloid Interface Sci. 74 (1980) 227–243.
[38] U. Schwertmann, H. Fechter, Clay Miner. 29 (1994) 87–92.
[39] J.-M.R. Génin, R. Aïssa, A. Géhin, M. Abdelmoula, O. Benali, V. Ernstsen, G. Ona-Nguema, C. Upadhyay, Ch. Ruby, Solid State Sci. 7 (2005) 545–572.
[40] C. Domingo-Pascual, R. Rodríguez-Clemente, M.A. Blesa, Colloids Surf. A 79 (1993) 177–189.
[41] T. Hiemstra, W.H. van Riemsdijk, G.H. Bolt, J. Colloid Interface Sci. 133 (1989) 91–104.
[42] T. Hiemstra, J.C.M. de Wit, W.H. van Riemsdijk, J. Colloid Interface Sci. 133 (1989) 105–117.
[43] M.G. Kim, S.B. Lee, J. Mol. Catal. B 2 (1996) 127–140.
[44] M.G. Bellino, A.E. Regazzoni, G.J.A.A. Soler-Illia, ACS Appl. Mater. Interfaces 2 (2010) 360–365.
[45] R. Reshmi, G. Sanjay, S. Sugunan, Catal. Commun. 8 (2007) 393–399.